

SPACE VLBI OBSERVATIONS OF 3C 371

JOSÉ-LUIS GÓMEZ

Instituto de Astrofísica de Andalucía, CSIC, Apartado 3004, 18080 Granada, Spain

AND

ALAN P. MARSCHER

Department of Astronomy, Boston University, 725 Commonwealth Avenue, Boston, MA 02215, USA

Draft version October 30, 2018

ABSTRACT

We present the first space VLBI observations of 3C 371, carried out at a frequency of 4.8 GHz. The combination of the high resolution provided by the orbiting antenna Highly Advanced Laboratory for Communications and Astronomy (HALCA) and the high sensitivity of the VLBA allows imaging of the jet of 3C 371 with an angular resolution of approximately 0.26 mas, which for this relatively nearby source corresponds to $\sim 0.4 h^{-1}$ pc. Comparison between two epochs separated by 66 days reveals no apparent motions in the inner 7 mas jet structure above an upper limit of $\sim 1.4 h^{-1} c$. This value, the absence of detectable counterjet emission from the presumably symmetric jet, plus the presence of extended double-lobe structure, are consistent with the knots in the jet being stationary features such as standing shocks. The jet intensity declines with the angular distance from the core as $\phi^{-1.68}$. This is more gradual than that derived for 3C 120, $\phi^{-1.86}$, for which there is evidence for strong interactions between the jet and ambient medium. This suggests that in 3C 371 there is a greater level of *in situ* acceleration of electrons and amplification of magnetic field. We interpret sharp bends in the jet at sites of off-center knots as further evidence for the interaction between the jet and external medium, which may also be responsible for the generation of standing recollimation shocks. These recollimation shocks may be responsible for the presumably stationary components. The radio properties of 3C 371 are intermediate between those of other radio galaxies with bright cores and those of BL Lacertae objects.

Subject headings: Techniques: interferometric - galaxies: active - BL Lacertae objects: individual: 3C 371 - Galaxies: jets - Radio continuum: galaxies

1. INTRODUCTION

The radio source 3C 371 has been identified with an N galaxy by Wyndham (1966) at a redshift of 0.05 (Sandage 1967). The spectrum of this object shows emission lines similar to those found normally in giant E galaxies, but with a highly variable nonthermal continuum, which has led to its classification as a BL Lacertae object (Miller 1975). 3C 371 has been observed to be variable at a variety of wavelengths: radio (Aller, Aller, & Hughes 1992), ultraviolet (Edelson 1992), optical (Carini, Nobel, & Miller 1998), and X-rays (Worrall et al. 1984).

Very Long Baseline Interferometry (VLBI) observations of 3C 371 have shown a complex milliarcsecond scale jet extending to the west (Pearson & Readhead 1981, 1988; Lind 1987; Polatidis et al. 1995; Kellerman et al. 1998). Polarimetric 5 GHz VLBI observations by Gabuzda et al. (1989) revealed very low polarization for the core ($\leq 0.3\%$), uncharacteristic of BL Lacertae objects. This, together with its low bolometric luminosity (Impey et al. 1984), led them to suggest that 3C 371 may be a transitional object between BL Lacertae and emission line objects. Very Large Array (VLA) arcsecond resolution images (O’Dea, Barvainis, & Challis 1988; Wrobel & Lind 1990; Stanghellini et al. 1997) show a partially bent jet with a magnetic field aligned with the jet direction. High dynamic range 5 GHz VLA images by Wrobel & Lind (1990) have revealed twin lobes, a hot spot, and large radio halo, unusual characteristics for a BL Lacertae object. An optical jet associated with 3C 371 has also been reported by Nilsson et al. (1997), who detected

a bright knot at $3''$ from the nucleus, coincident with that observed at radio wavelengths by Aukjor et al. (1994). Nilsson et al. interpreted this as evidence for interaction between the jet and the external medium.

We present here the first VLBI Space Observatory Program (VSOP) observations of 3C 371. VSOP observations are performed using a ground array of radio telescopes and the Japanese orbiting 8 meter antenna HALCA (Highly Advanced Laboratory for Communications and Astronomy). The satellite has an orbital period of approximately 6 hours, with apogee of 21000 km and perigee of 560 km. Data from HALCA are transmitted to a ground network of 5 tracking stations, where they are recorded and subsequently correlated with the data from the participating ground antennas.

2. OBSERVATIONS AND DATA REDUCTION

VSOP observations of 3C 371 were performed on 1998 March 11 (1998.19) and 1998 May 16 (1998.37) at a frequency of 4.8 GHz. NRAO’s¹ Very Long Baseline Array (VLBA) provided the ground array for both observations (with the exception of the St. Croix antenna, which did not participate in the May observation). The data were recorded in VLBA format with two intermediate-frequency bands (IF), centered on 4.800 and 4.816 GHz, each with a bandwidth of 16 MHz, and correlated in Socorro. The total durations of the observations were 9.5 (March) and 8 (May) hr, each covering somewhat longer than one HALCA orbit. Figure 1 shows the *uv*-coverage

¹The National Radio Astronomy Observatory is a facility of the National Science Foundation operated under cooperative agreement by Associated Universities, Inc.

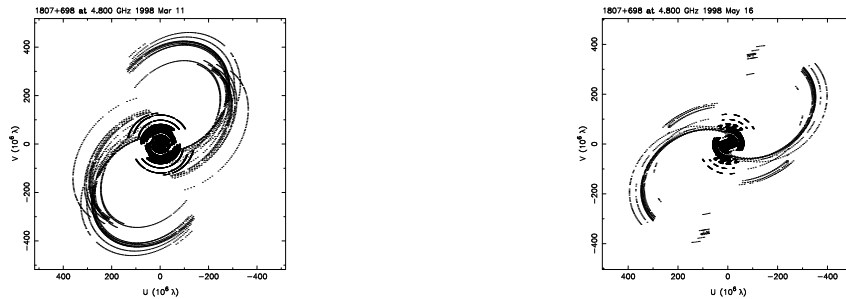


FIG. 1.— The uv -coverage corresponding to VLBA+HALCA observations of 3C 371 on 1998 March 11 (*left*) and 1998 May 16 (*right*).

obtained for each epoch, where the baselines to HALCA are clearly visible, providing an improvement in the resolution by more than 3 times that obtained using only the ground telescopes. Since the observational resolution is proportional to the frequency of observation, similar values can also be obtained by ground arrays at shorter wavelengths.

The reduction of the data was performed within the NRAO Astronomical Image Processing System (AIPS) software. Data with very discrepant amplitudes and/or phases on all baselines to a given antenna were deleted. Fringe fitting was performed to solve for the residual delay and fringe rate, resulting in good solutions for most of the HALCA data. After averaging all frequency channels the data were exported into the software DIFMAP (Shepherd 1997). An initial time average of 10 seconds was introduced prior to phase calibration with a point source model. A further time average of 2 minutes was introduced before imaging.

Imaging was performed through successive cleaning and self-calibration of the data, both in phase and amplitude. In order to study the inner milliarcsecond structure of 3C 371 with the highest resolution provided by VSOP, we imaged the data using uniform weighting. The more extended structure was revealed by making use of the ground data only, and with natural weighting.

3. RESULTS

Figure 2 shows the uniformly weighted VSOP and naturally weighted VLBA images obtained for 3C 371 at 1998 March 11 and 1998 May 16. Components in the total intensity images were analyzed by model fitting the uv data with elliptical Gaussian components within DIFMAP. Because of the smooth jet structure and non uniformity of the uv -coverage (see Fig. 1), model fitting was rather complicated. Owing to the difficulty of using model fitting to reproduce both very compact and more extended structure, we adopted the following approach. Starting with the hybrid map delta-function model, we deleted components within 7 mas of the core and then reconstructed the inner jet by model fitting with elliptical Gaussian components. Because of the complex structure of knots *K1* and *K2* in the outer region, model fitting of these components was accomplished by removing the delta-function components within the highest contour levels surrounding their respective positions, then model fitting the residuals with single elliptical Gaussians for each component. We have estimated the positional errors in the model fitting by introducing small changes in the position and studying the variations in the χ^2 of the fit, as well as by re-

producing the model fitting from the beginning and comparing with previous results. This yielded uncertainties of ~ 0.05 mas for the inner components *A* through *D*, and ~ 0.1 mas for knots *K1* and *K2*. Table 1 summarizes the physical parameters obtained for 3C 371 at both epochs. Tabulated data correspond to flux density (S), separation (r) and structural position angle (θ) relative to the core, FWHM major axis of the elliptical Gaussian component (a), ratio of minor to major axis (b/a), and position angle of the major axis (Φ).

3.1. Proper Motions

The possible existence of superluminal motions in the jet of 3C 371 is controversial owing to the different values estimated by several authors. Worrall et al. (1984) fit the total millimeter to X-ray spectrum of 3C 371 to the synchrotron-self-Compton jet model of Königl (1981), obtaining a lower limit of 10 for the Doppler beaming factor, $\delta_{\min} = 1/[\Gamma(1 - \beta \cos\theta)]$, where β is the bulk flow speed of the emitting plasma in units of c , $\Gamma = (1 - \beta^2)^{-1/2}$, and θ is the angle between the jet axis and the line of sight. Under the assumption that $\sin\theta = 1/\Gamma$, they predicted superluminal motion with values larger than $10 h^{-1}c$ ($H_0 = 100 h \text{ km s}^{-1} \text{ Mpc}^{-1}$). Similar values were suggested by Lind (1987) through the analysis of two 5 GHz VLBI images obtained in 1982 and 1985. A study of the changes in brightness distribution led these authors to conclude that the apparent speeds were between 6 and $7 h^{-1}c$.

However, VLA observations by Wrobel & Lind (1990) show that the morphology of the extended radio emission of 3C 371 is that of a double-lobed radio source. Since the lobes do not overlap, the viewing angle cannot be extremely small. On the other hand, they detected no counterjet, which suggests that the source does not lie near the plane of the sky. It is therefore difficult to obtain an agreement between the large viewing angle estimated by Wrobel & Lind (1990), and the large apparent motions of Worrall et al. (1984) and Lind (1987), since apparent motions of the order of 10 would require a viewing angle smaller than approximately 6° . Thus, a direct determination of the apparent proper motion is of special importance for interpreting this source.

The VLBA natural-weighted images of Fig. 2 show a jet extending to the west-southwest over about 60 mas. Superimposed on the homogeneous jet brightness distribution, knots *K1* and *K2* appear at ~ 12 and 26 mas from the core. The computed apparent motions of 1.2 and 0.3 mas/yr (2.8 and $0.7 h^{-1}c$) for *K1* and *K2*, respectively, lie within the estimated errors. We therefore obtain an upper limit to the apparent velocity of the

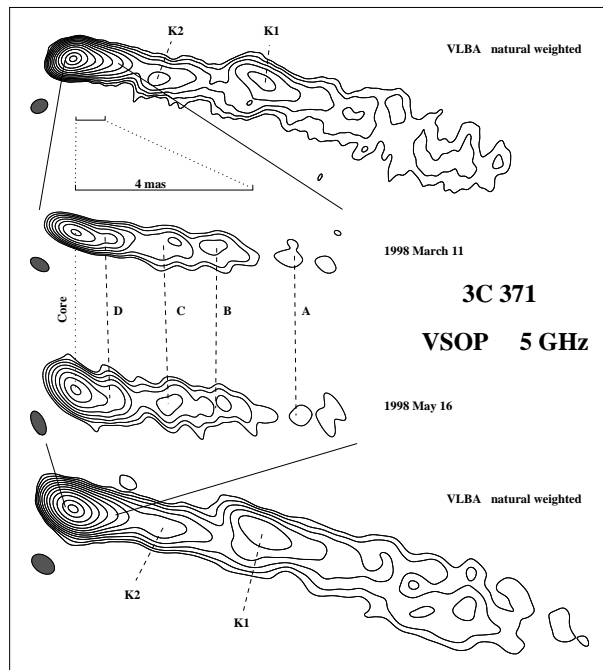


FIG. 2.— VSOP total intensity images of 3C 371 at 5 GHz obtained on 1998 March 11 (*top middle image*) and 1998 May 16 (*bottom middle image*). Natural weighted images obtained using only the ground array (VLBA) data are shown, revealing the more extended jet structure. From top to bottom: Contour levels are in factors of 2, starting at 0.06, 0.7, 0.8, and 0.06% (adding 90% except for the March 1998 VSOP image) of the peak intensity of 625, 331, 283, and 674 mJy beam⁻¹. Convolution beams (shown as filled ellipses) are 2.4×1.79 , 0.457×0.257 , 0.576×0.279 , and 3.45×2.3 mas, with position angles of 59° , -62° , 25° , and 55° .

large scale jet structure of $\sim 3 h^{-1}c$. Comparison with previous 5 GHz VLBI maps by Lind (1987) obtained in 1982 and 1985 reveals a tentative identification of *K1* and *K2* with their components *C* and *E*, respectively, in which case both components would have remained stationary over a 15-yr period, in discrepancy with the value of $7 h^{-1}c$ estimated by Lind (1987).

The VSOP images of Fig. 2 reveal up to four distinct components, mapped with an angular resolution of ~ 0.26 mas, which for this nearby source corresponds to a linear resolution of $\sim 0.4 h^{-1} pc$. The apparent velocities for components *A* through *D* range between 0.4 and $1.2 h^{-1}c$. However, the relatively large errors in the model fitting of this complex source (see also Gabuzda et al. 1989) lead to an estimated error in the apparent motion of $\sim 1.4 h^{-1}c$, and therefore we can only conclude that any motions in the inner structure of 3C 371 must be smaller than this uncertainty.

4. DISCUSSION AND CONCLUSIONS

Our rather low upper limit to the apparent velocity of the inner jet requires that either (1) the Lorentz factor is low, (2) the viewing angle is large, (3) the Lorentz factor is high but the viewing angle is small, $\theta \ll \Gamma^{-1}$, or (4) the knots in the jet are stationary features. We assume that the absence of counterjet emission in the images of Fig. 2 is due to beaming of an otherwise symmetric twin jet, and estimate a minimum observed jet:counterjet emission ratio of $\sim 1700 : 1$ (peak flux:noise level). In the case of *optically thin* emission in a steady-state jet with randomly oriented magnetic field, this ratio is given by $[(1 + \beta \cos \theta)/(1 - \beta \cos \theta)]^{2-\alpha}$, where α is the spectral index ($S_\nu \propto \nu^\alpha$); $\alpha = -0.03$ in 3C 371 (Taylor et al.

1996). We note that for jet regions with relatively large opacity, such as the brightest region of the radio core, the above equation is not valid, and the jet:counterjet flux ratio is significantly smaller than that obtained using the previous equation. Therefore, the use of this equation provides a lower limit to the flow Lorentz factor, and a corresponding upper limit to the viewing angle. Solving the jet:counterjet flux ratio equation gives $\beta \cos \theta > 0.95$, or $\beta \geq 0.95$ ($\Gamma \geq 3.2$) and $\theta \leq 18^\circ$. Hence, if the jet is symmetric, we can eliminate possibilities (1) and (2). Option (3) seems unlikely, since the twin-lobe extended radio structure (Wrobel & Lind 1990) is not easily explained if the viewing angle is much less than $\theta \sim 18^\circ$. Hence, we conclude that option (4) is the most plausible, especially if we consider the previously mentioned opacity effects in the determination of the jet:counterjet flux ratio. Further strong evidence supporting the idea that the components may be stationary features comes from the comparison with images of similar resolution obtained by Kellerman et al. (1998) using the VLBA at 15 GHz (see <http://www.cv.nrao.edu/2cmsurvey>). These images show a knotty jet with only minor structural changes during the four years covered by their observations, and resembles the structure of Fig. 2.

Similar to the radio galaxy 3C 120 (Walker 1997; Gómez et al. 1998), the jet of 3C 371 displays a gentle curvature. Sharper bends are observed farther downstream of the emission shown in Fig. 2 (Wrobel & Lind 1990; Akujor et al. 1994); these have been interpreted as the interaction of the jet with the external medium (Nilsson et al. 1997). The fact that knots *K1* and *K2* are offset with respect to the jet ridge line supports this interpretation. They may arise from Kelvin-Helmholtz instabilities (as seems to be the case in 0836+710; Lobanov et al. 1998),

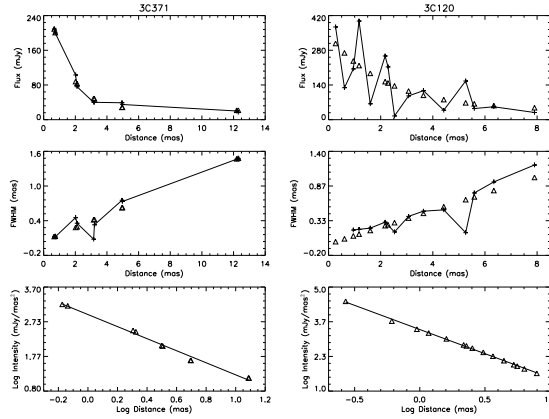


FIG. 3.— Flux density (*top*) and FWHM angular size (*middle*) vs. angular distance of the components in 3C 371 (*left*) and 3C 120 (*right*, from Gómez, Marscher, & Alberdi 1999). Data for component *KI* is neglected since the component does not fill the entire jet width. Sizes of components in 3C 120 for which no estimation of the FWHM have been obtained are ignored. The data are represented by crosses. Triangles correspond to the fitted exponential decay for the flux density, and linear fit for the FWHM. Jet intensity decays with angular distance as $\phi^{-1.68}$ for 3C 371 and $\phi^{-1.86}$ for 3C 120 (*bottom* plots).

or perhaps some other consequence of strong interactions with the external medium (cf. 3C 120; Gómez, Marscher, & Alberdi 1999). If the jet of 3C 371 is confined by the pressure of the external medium, the slow motion (consistent with no motion) observed in components *D* through *A* suggests that these components may be associated with recollimation shocks. Numerical simulations by Gómez et al. (1995, 1997) show that the enhancement of specific internal energy and rest-mass density at internal oblique shocks results in the appearance of a regular pattern of knots of high emission. The separation and strength of the knots is a function of the jet opening angle and Mach number.

The images allow us to measure the gradient in intensity of the jet. For that we have represented in Fig. 3 the flux density and the FWHM angular size of the components in 3C 371, for both epochs, as a function of the distance along the jet. The flux density evolution can be fitted to an exponential function of exponent -0.77 , while for the component sizes a linear fit gives a jet opening half-angle of 3.3° . We have neglected the data corresponding to component *KI*, since at this position the jet seems considerable wider than its estimated FWHM. Using these fits, we have interpolated the flux and jet width at the position of the components, obtaining a jet intensity which decays with angular distance ϕ from the core as $\phi^{-1.68}$, shown in Fig. 3. For comparison, we have performed a similar analysis for the jet in 3C120 using the data in Gómez, Marscher, & Alberdi (1999). In this case, the flux decays with an exponent of -0.45 , and the jet half opening angle is 3.7° . The intensity is found to decay as $\phi^{-1.86}$. The flatter gradient in the case of 3C 371 suggests that in

this object there is a greater level of *in situ* acceleration of electrons and amplification of magnetic field than for 3C 120, for which Gómez, Marscher, & Alberdi (1999) found evidence of strong interactions between the jet and ambient medium. This would lead to the physical conditions (high energy electrons and acceleration) necessary in order to explain the optical jet observed in this source (Nilsson et al. 1997). It would also imply that the jet of 3C 371 undergoes greater interaction with the external medium, which is a likely source of the shock waves and turbulence that could cause this amplification. As discussed above, such interactions with the external medium would also excite standing shocks in the jet, leading to the appearance of stationary components.

The properties of 3C 371 indicate that this source may be a hybrid of a BL Lac object and a radio galaxy. That is, it may represent a BL Lac object observed at a somewhat wider viewing angle than is normally the case. The radio galaxy aspects of such an object should then become at least partly apparent, as indeed occurs in 3C 371. It would be of great interest to make higher frequency VLBI observations of this source, especially with polarization, in order to investigate possible motions closer to the central engine and to test whether indeed 3C 371 can be considered a true transitional object.

This research was supported in part by Spain's Dirección General de Investigación Científica y Técnica (DGICYT) grant PB97-1164, by NATO travel grant SA.5-2-03 (CRG/961228), and by U.S. National Science Foundation grant AST-9802941.

REFERENCES

- Akujor, C. E., Lüdke, E., Browne, I. W. A., Leahy, J. P., Garrington, S. T., Jackson, N., & Thomasson, P. 1994, *A&AS*, 105, 247
 Aller, M. F., Aller, H. D., & Hughes, P. A. 1992, *ApJ*, 399, 16
 Carini, M. T., Noble, J. C., & Miller, H. R. 1998, *AJ*, 116, 2667
 Edelson, R. 1992, *ApJ*, 401, 516
 Gabuzda, D. C., Cawthorne, T. V., Roberts, D. H., & Wardle, J. F. C. 1989, *ApJ*, 347, 701
 Gómez, J. L., Martí, J. M., Marscher, A. P., Ibáñez, J. M., & Marcaide, J. M. 1995, *ApJ*, 449, L19
 Gómez, J. L., Martí, J. M., Marscher, A. P., Ibáñez, J. M., & Alberdi, A. 1997, *ApJ*, 482, L33
 Gómez, J. L., Marscher, A. P., Alberdi, A., Martí, J. M., & Ibáñez, J. M. 1998, *ApJ*, 499, 221
 Gómez, J. L., Marscher, A. P., Alberdi, A. 1999, *ApJ*, 521, L29
 Impey, C. D., Prand, P. W. J. L., Wolstencroft, R. D., & Williams, P. M. 1984, *MNRAS*, 209, 245
 Kellerman, K. I., Vermeulen, R. C., Zensus, J. A., & Cohen, M. H. 1998, *AJ*, 115, 1295
 Königl, A. 1981, *ApJ*, 243, 700

TABLE 1
PHYSICAL PARAMETERS OF 3C 371

Comp.	S (mJy)		r (mas)		θ ($^{\circ}$)		a (mas)		b/a		Φ ($^{\circ}$)	
	1998.19	1998.37	1998.19	1998.37	1998.19	1998.37	1998.19	1998.37	1998.19	1998.37	1998.19	1998.37
Core .	444	469	0.38	0.45	0.17	0.18	75	78
D	209	200	0.67	0.73	-102	-104	0.61	0.69	0.27	0.22	-87	-85
C	103	76	2.02	2.11	-99	-98	1.11	0.72	0.52	0.63	83	-70
B	40	40	3.21	3.16	-97	-97	0.79	1.01	0.53	0.10	41	-84
A	39	35	4.95	4.98	-97	-97	2.34	2.33	0.41	0.40	82	82
K2 . . .	20	17	12.2	12.3	-103	-102	3.27	2.75	0.57	0.68	88	62
K1 . . .	15	16	26.5	26.4	-97	-97	2.76	2.41	0.57	0.75	57	69

Lind, K. R. 1987, in Superluminal Radio Sources, ed. J. A. Zensus, & T. J. Pearson (Cambridge Univ. Press), 180
 Lobanov, A. P., Krichbaum, T. P., Witzel, A., Kraus, A., Zensus, J. A., Britzen, S., Otterbein, K., Hummel, C. A., & Johnston, K. 1998, A&A, 340, L60
 Miller, J. S. 1975, ApJ, 200, L55
 Nilsson, K., Heidt, J., Pursimo, T., Sillanpää, A., Takalo, L. O., & Jäger, K. 1997, ApJ, 484, L107
 O'Dea, C. P., Barvainis, R., & Challis, P. 1988, AJ, 96, 435
 Pearson, T. J., & Readhead, A. C. S. 1981, ApJ, 248, 61
 Pearson, T. J., & Readhead, A. C. S. 1988, ApJ, 328, 114
 Polatidis, A. G., Wilkinson, P. N., Xu, W., Readhead, A. C. S., Pearson, T. J., Taylor, G. B., & Vermeulen, R. C. 1995, ApJS, 98, 1

Sandage, A. 1967, ApJ, 150, L177
 Shepherd, M. C. 1997, in Astronomical Data Analysis Software and Systems VI, Astron. Soc. Pac. Conf. Proc., 125
 Stanghellini, C., Dallacasa, D., Bondi, M., & Della Ceca R. 1997, A&A, 325, 911
 Taylor, G. B., Vermeulen, R. C., Readhead, A. C. S., Pearson, T. J., Henstock, D. R., & Wilkinson, P. N. 1996, ApJS, 107, 37
 Walker, R. C. 1997, ApJ, 488, 675
 Worrall, D. M., et al. 1984, ApJ, 284, 512
 Wrobel, J. M., & Lind, K. R. 1990, ApJ, 348, 135
 Wyndham, J. D. 1966, ApJ, 144, 459